Open Access Online Journal on Astronomy and Astrophysics

Acta Astrophysica Taurica

www.astrophysicatauricum.org

Acta Astrophys. Tau. 5(3), 14–17 (2024)

Cyclic variations in the areas of coronal holes and sunspots in 2010–2021

O.A. Andreeva, V.I. Abramenko, V.M. Malashchuk

Crimean Astrophysical Observatory, Nauchny 298409
e-mail: olga@craocrimea.ru

Received 3 November 2021

ABSTRACT

The paper investigates a cyclic relation between coronal holes (CHs) and solar activity (SA) indices. Based on observational data obtained with the SDO/AIA instrument in the Fe XII 19.3 nm line between May 13, 2010 and May 13, 2021, the properties of polar and nonpolar coronal holes are studied. The features of each group are considered in detail, and the relationship of CH areas with the phase of the solar cycle is established. During the period under study, a north-south (N-S) asymmetry of the hemispheres was detected both in the SA indices and in the localization of the maximum areas of polar and nonpolar CHs. The determining role of polar CHs of the southern hemisphere and nonpolar CHs of the northern hemisphere was revealed throughout the cycle, which manifested itself in the SA dynamics of the hemispheres and the solar disk as a whole.

Key words: Sun, solar cycle, sunspots, coronal holes

1 Introduction

The solar corona is a source of very dynamic events (flares, coronal mass ejections, solar wind, etc.), which mainly occur in active regions (ARs) and coronal holes (CHs). A close relation between these phenomena has been noted repeatedly (Bohlin, Sheeley, 1978; Sheeley, Harvey, 1981), and the role of ARs in the formation and subsequent evolution of CHs is beyond doubt. However, the mechanism of the origin and evolution of polar, mid-, and low-latitude CHs is not fully understood. In the standard solar dynamo model (see, for example, Hoyng, 1993), the initially dipole poloidal field at solar minimum is transformed by differential rotation into a strong toroidal field observed at solar maximum. During the minimum of activity, the open field regions above the poles (polar coronal holes) reach their maximum expansion, and the number of low-latitude regions of closed, strong field (active regions and sunspots) is minimal. As the activity cycle develops, more and more sunspots appear, and the polar coronal holes become smaller. Small low-latitude coronal holes appear at this time, but the total area of the Sun covered by coronal holes decreases as the number of sunspots increases. The relationship between these two manifestations of the Sun's magnetic evolution was first investigated by Bravo, Otaola (1989). Later, Bravo, Stewart (1994, 1997) showed that there is a close relation between the evolution of polar coronal hole areas, estimated from K-coronameter observations, and the sunspot number. Akhtemov et al. (2020) note that nonpolar CHs can make a significant contribution to the solar mean magnetic field. This suggests a close relation of nonpolar CHs with the global solar dynamo action.

It is generally accepted that the indices of solar activity – sunspot numbers (SSN) and areas (Ssp) – reflect the 11-year solar cyclicity and, consequently, are associated with the solar dynamo action. On the other hand, coronal holes are regions of the open flux and also reflect the solar dynamo action. To statistically investigate the relationship between coronal holes and sunspots, we consider the cyclic variations of their areas. This work continues a series of works by Andreeva et al. (2020), Andreeva, Malashchuk (2020) and others on the study of CHs based on SDO/AIA observations.

2 Observational data, statistics and research methods

Our study is based on observational data obtained over 11 years by the Atmospheric Imaging Assembly (AIA) instrument on board the Solar Dynamics Observatory (SDO) in the Fe XII 19.3 nm line (SolarMonitor.org website[1]). Since these data were not available at the beginning of cycle 24, we limited ourselves to the period from May 13, 2010 to May 13, 2021. The exact location of such large-scale objects as CHs can be determined by applying image processing methods to extreme ultraviolet (EUV) data. To identify CHs and determine their areas, we used the Heliophysics Event Knowledgebase (HEK)[2] (Hurlburt et al., 2012). Information on CHs was found using a set of multichannel fuzzy

[1] https://solarmonitor.org/index.php
[2] http://www.lmsal.com/hek/hek_isolsearch.html

clustering algorithms SPoCA (Spatial Possibilistic Clustering Algorithm) described in detail in Barra et al. (2009) and Verbeeck et al. (2014). They automatically segment solar EUV images into a set of functions. SPoCA identifies ARs, quiet Sun, and CHs by minimizing the fuzzy intraclass variance, performs segmentation up to $0.99R_{\odot}$, excluding structures outside the disk. Using the HEK, we created an array of daily total coronal hole areas for the period between 13.05.2010 and 13.05.2021, expressed in Mm^2. In the course of the study, we analyzed 17 717 CHs, less than 7 % of which crossed the equator. We assumed that the area of a CH crossing the equator is divided into two parts, and each of them belongs to the corresponding hemisphere, depending on its location. In our opinion, we did not make a big mistake because there were quite a few such CHs. Taking this assumption into account, 9064 CHs were observed in the N-hemisphere and 8653 in the S-hemisphere. As in our earlier works, here we investigate two groups of CHs: polar (CH_pol) and nonpolar (CH_nonpol). CH_pol start at the poles, i.e., at a latitude of 90 degrees, and descend, depending on their development and phase of the cycle, sometimes to middle and even low latitudes. CH_nonpol are mid- and low-latitude CHs not associated with the pole. The division of CHs into two groups, which we adopted in our study, is described in detail in Andreeva et al. (2020). Table 1 provides statistical data on the processing of CHs in the period from 13.05.2010 to 13.05.2021.

Table 1 shows that the statistical volume of the presented material is quite extensive and provides a basis for studying the relationship between cyclic variations of different types of CHs and solar activity indices (SSN and Ssp).

3 Cyclic variations of coronal hole and sunspot areas

3.1 Variations of solar activity indices

Figures 1 and 2 show variations of solar activity indices SSN and Ssp in the period from 13.05.2010 to 13.05.2021. In all graphs of these figures and further in Fig. 3, thin gray curves are the daily total values of the corresponding quantities; thick colored curves against their background are data smoothed over half a year.

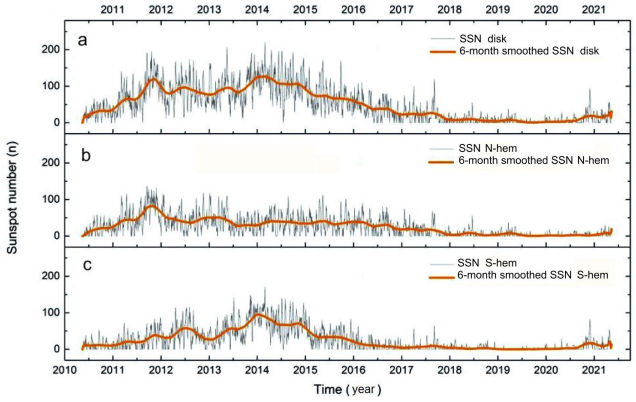

Fig. 1. Variations of the sunspot number index in the period from 13.05.2010 to 13.05.2021 for the entire solar disk (a), for the N- (b) and S- (c) hemispheres.

The data on SSN and Ssp are taken from the WDC-SILSO[3] and Solar Cycle Science[4] websites. Both indices show a similar trend in the dynamics of the cyclic distribution of sunspot formation. Both figures show a north-south asymmetry in the distribution of indices. It is known that there were two peaks of solar activity maximum in cycle 24. It can be seen that the first peak (2012) is determined by the northern hemisphere, and the second peak (2014) is caused by the sunspot activity of the southern hemisphere. For our

[3] https://wwwbis.sidc.be/silso/datafiles
[4] http://solarcyclescience.com/AR_Database/daily_area.txt

Table 1. Statistics on the processing of coronal holes in the period from 13.05.2010 to 13.05.2021.

Years	2010	2011	2012	2013	2014	2015	2016	2017	2018	2019	2020	2021	**Total**
Observation days	233	364	366	365	365	365	357	365	365	365	366	133	4009
CH_s N-hem	418	539	1072	1336	1059	887	887	806	740	577	536	207	9064
CH_s S-hem	387	724	1189	1055	1041	855	707	685	628	597	545	240	8653
CH_s N_S_eq	23	107	270	190	117	174	96	102	78	17	0	8	1182
CH_s N_pol	190	229	230	203	301	251	411	452	485	495	478	163	3888
CH_s S_pol	267	409	375	171	289	397	364	425	437	506	501	150	4291
CH_s N_nonpol	228	310	842	1133	758	636	476	354	255	82	58	44	5176
CH_s S_nonpol	120	315	814	884	752	458	343	260	191	91	44	90	4362
All CH_s	805	1263	2261	2391	2100	1742	1594	1491	1368	1174	1081	447	17717

Note. The top row lists the years of the period under study. The second row shows the number of CH observation days analyzed in each year. Below is the annual information on the number of CHs for the northern (CHs N-hem) and southern (CHs S-hem) hemispheres, as well as the number of CHs crossing the equator (CHs N_S_eq). The following rows of Table 1 provide annual statistics on the number of polar (CHs N_pol, CHs S_pol) and nonpolar (CHs N_nonpol, CHs S_nonpol) CHs for the northern and southern hemispheres, respectively. The bottom row (All CHs) is the total annual number of CHs recorded on the entire visible surface of the Sun. The right column (Total) reflects the total number of values corresponding to each row for the entire period under study.

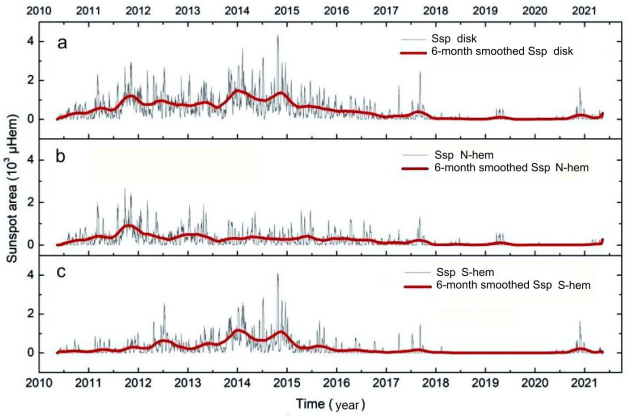

Fig. 2. Variations of sunspot areas in the period from 13.05.2010 to 13.05.2021 for the entire solar disk (a), for the N- (b) and S- (c) hemispheres.

task, we regarded it more physical to compare the areas of CHs (Sch) with the second SA index – the areas of sunspots.

3.2 Variations of daily total areas of CHs

Temporal variations of the daily total areas of CHs for the studied period are presented in Fig. 3. We examined the cyclic variations of CHs on the entire visible surface of the solar disk, separately in each hemisphere, and the contribution of the two types of CHs to the overall SA dynamics in the period under consideration. This is reflected in panels (a – e) of Fig. 3. Here it should be noted that the visible quasiperiodic oscillations in Fig. 3b, c are an artifact caused by the inclination of the Sun's rotation axis. It manifests itself in the hemispheres and is absent in the total areas of CHs over the entire disk (Fig. 3a). It can be seen that throughout the cycle, the hemispheres behaved differently. There are pronounced peaks of dominance of the hemispheres in terms of CH areas. In the rising phase in 2011–2012 and in 2015, the southern hemisphere led in terms of the maximum CH areas. In the second maximum and on the declining branch, the northern hemisphere prevailed.

Figure 3d, e shows the division of all areas of the studied CHs into the areas of polar (Sch_pol) and nonpolar (Sch_nonpol) CHs. There are two maxima of Sch_pol occurring in 2011–2012 and 2015, which are the phases of growth and decline of SA. After the decline phase and at the minimum of cycles 24–25, the total areas of polar CHs approach the average level of values, which is about 14×10^4 Mm^2. At the same time, the maxima of Sch_nonpol are consistent with the phase of the second maximum of cycle 24 in 2013–2014. The total areas of nonpolar CHs at the beginning of the studied period can be seen to have low values, whereas at the decline and minimum of cycles 24–25 they practically disappear and appear on the rising branch of cycle 25. They also repeat the cycle, as shown in panels (a) of Figs. 1 and 2 for sunspots.

While in the rising phase and the first maximum in the northern hemisphere all Sch (Fig. 3b) were minimal, the sunspot activity was pronounced (see Figs. 1b and 2b). Interestingly, however, and we noted this in our earlier works

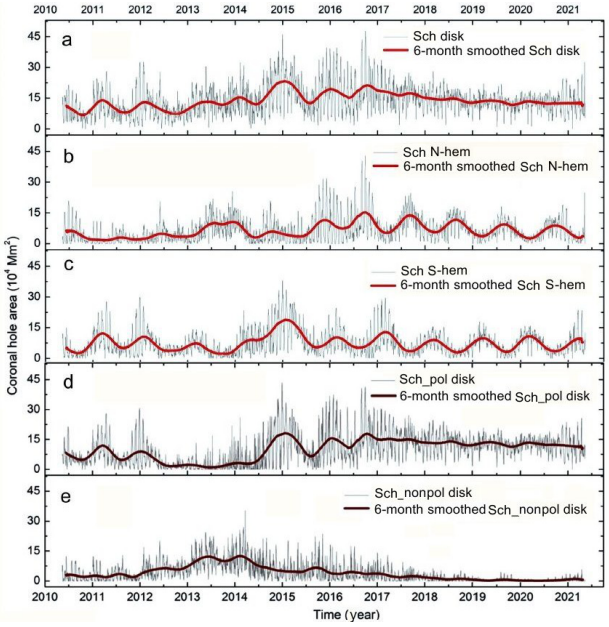

Fig. 3. Variations of the daily total areas of CHs in the period from 13.05.2010 to 13.05.2021. The panels from top to bottom show (a) Sch of the entire visible surface of the Sun; Sch of the N- (b) and S- (c) hemispheres; Sch of all polar (d) and all nonpolar (e) CHs of the visible surface of the Sun.

(Andreeva, Malashchuk, 2020) where we did not yet divide CHs into polar and nonpolar: in the second maximum and on the declining branch of 2014–2015, the southern hemisphere led both in Sch (see Fig. 3c) and in SSN and Ssp (panels (c) of Figs. 1 and 2).

3.3 Variations of areas of two types of coronal holes and sunspots in the hemispheres

In the course of studying the relationship between CHs and sunspots, we considered the contribution of polar and nonpolar CHs to the SA dynamics throughout the cycle. Next, we compared the cyclic variations of Sch_pol, Sch_nonpol, and Ssp. Figure 4 shows the time variation of the areas of polar and nonpolar CHs as well as the areas of sunspots for the two hemispheres.

While in the first maximum of 2012 the northern hemisphere led in terms of sunspot areas (Fig. 4a), Sch_pol were minimal almost until the beginning of the declining phase of cycle 24 (October 2014). The southern hemisphere (Fig. 4b) led in terms of sunspot areas in the second maximum, whereas the maxima of Sch_pol were observed in the phases of growth, decline, and minimum of SA. Ssp are minimal at the beginning of the cycle, after the decline phase, and at the minimum of SA (red curves in Fig. 4a, b), whereas Sch_pol have fairly high stable values (blue curves in Fig. 4a, b).

The daily total area of polar CHs increases at the minima of solar activity and decreases at the maximum of the cycle.

For nonpolar CHs in both hemispheres (brown curves in Fig. 4a, b), there is a tendency for areas to increase in the phase of growth and maximum of SA and to decrease in the phases of decline and minimum.

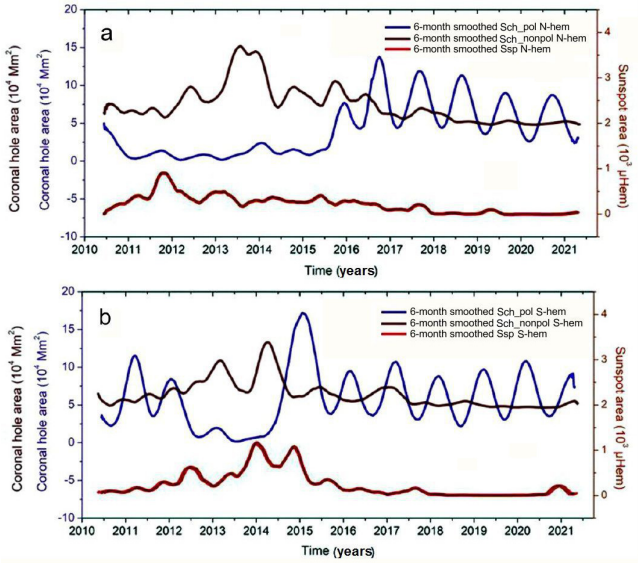

Fig. 4. Variations of the areas of two types of CHs and sunspots in the period from 13.05.2010 to 13.05.2021 in the N- (a) and S- (b) hemispheres. The areas of polar and nonpolar CHs are shown in blue and brown, respectively, and the areas of sunspots are shown in red.

From the two panels of Fig. 4, one can see some interesting patterns in the dominance of each type of CHs in different hemispheres. Thus, for example, the *determining role of polar CHs in the southern hemisphere* is clearly visible (blue curve in Fig. 4b). Bright peaks around 2011, 2012, and 2015 are repeated in the patterns of the total area of *all polar CHs*, *all CHs of the southern hemisphere*, and *all CHs of the visible surface of the solar disk* (see Fig. 3d, c, and a, respectively). On the other hand, one can note the *special role of nonpolar CHs in the northern hemisphere* (brown curve in Fig. 4a), whose area is large in 2013–2014. They are also repeated in the overall picture for *all nonpolar CHs*, *all CHs of the northern hemisphere*, and *all CHs of the visible surface of the solar disk* (Fig. 3e, b, a, respectively).

4 Results

We have examined in detail the behavior of *polar* and *nonpolar* coronal holes over the 11-year cycle. We have established a relation between the areas of coronal holes and the phase of the solar cycle. Analysis of the two types of coronal holes in the period from 13.05.2010 to 13.05.2021 shows the following findings:

1. The daily total area of *polar* coronal holes increases at the minima of solar activity and decreases at the maximum of the cycle. This is consistent with the general idea of polar coronal holes as the main source of the Sun's dipole magnetic field (Ikhsanov, Ivanov, 1999; Hess Webber et al., 2014; Bilenko, Tavastsherna, 2016).
2. Meanwhile, *nonpolar* coronal holes repeat the cycle. This once again confirms our assumption that the two types of CHs have different nature. *Nonpolar* CHs change quasisynchronously with the sunspot activity of the Sun, which allows one to suggest the presence of a physical relation between these two phenomena.
3. A north-south asymmetry of the hemispheres was found both in terms of solar activity indices and in terms of the localization of the maximum areas of *polar* and *nonpolar* CHs.
4. The determining role of *polar* CHs of the southern hemisphere and *nonpolar* CHs of the northern hemisphere was revealed, which manifested itself in the SA dynamics of the hemispheres and the Sun as a whole.

Acknowledgments. The authors express their gratitude to the referee for the support and interest in the paper and for a number of useful comments.

SDO is a project of NASA's Living With a Star program. SDO/AIA data were provided by the Joint Science Operation Center (JSOC). The authors are grateful to the Heliophysics Event Knowledgebase (HEK) project team for the opportunity to access the databases of CHs.

We also thank WDC-SILSO (Royal Observatory of Belgium, Brussels) for the opportunity to use data on sunspot numbers.

References

Andreeva A.O., Malashchuk V.M., 2020. Geomagnetism and Aeronomy, vol. 60, no. 8, pp. 1093–1100.

Andreeva O.A., Abramenko V.I. and Malaschuk V.M., 2020. Astrophysics, vol. 63, no. 1, pp. 114–124, doi:10.1007/s10511-020-09619-2.

Akhtemov Z.S., Tsap Y.T., Haneychuk V.I., 2020. Astrophysics, vol. 63, pp. 399–407.

Barra V., Delouille V., Kretzschmar M., Hochedez J.-F., 2009. Astron. Astrophys., vol. 505, pp. 361–371.

Bilenko I.A., Tavastsherna K.S., 2016. Solar Phys., vol. 291, pp. 2329–2352.

Bohlin J.D., Sheeley N.R., Jr., 1978. Solar Phys., vol. 56, pp. 125–151.

Bravo S., Otaola J.A., 1989. Solar Phys., vol. 122, pp. 335–443.

Bravo S., Stewart G.A., 1994. Solar Phys., vol. 154, pp. 377–384.

Bravo S., Stewart G.A., 1997. Solar Phys., vol. 173, no. 1, pp. 193–198.

Hess Webber S.A., Karna N., Pesnell W.D., Kirk M.S., 2014. Solar Phys., vol. 289, no. 11, pp. 4047–4067.

Hoyng P., 1993. Astron. Astrophys., vol. 272, pp. 321–339.

Hurlburt N., Cheung M., Schrijver C., et al., 2012. Solar Phys., vol. 275, pp. 67–78.

Ikhsanov R., Ivanov V., 1999. Solar Phys., vol. 188, pp. 245–258.

Sheeley N.R., Jr. & Harvey J.W., 1981. Solar Phys., vol. 70, pp. 237–249.

Verbeeck C., Delouille V., Mampaey B., De Visscher R., 2014. Astron. Astrophys., vol. 561, id A29.